Supplementary information for

Real-time monitoring of Ligand binding to G-Quadruplex and duplex DNA by whispering gallery mode (WGM) sensing

Sirirat Panich[†], Mazen Haj Sleiman[‡], Isobel Steer[‡], Sylvain Ladame[‡],[‡] and Joshua B. Edel *[†]*

[†]Department of Chemistry, Imperial College London, South Kensington Campus, London, SW7 2AZ.

[‡]Department of Bioengineering, Imperial College London, South Kensington Campus,
London, SW7 2AZ.

Corresponding Author

* E-mail joshua.edel@imperial.ac.uk; sladame@imperial.ac.uk

Phone: (+44 (0)20 7594 0754)

SI Contents

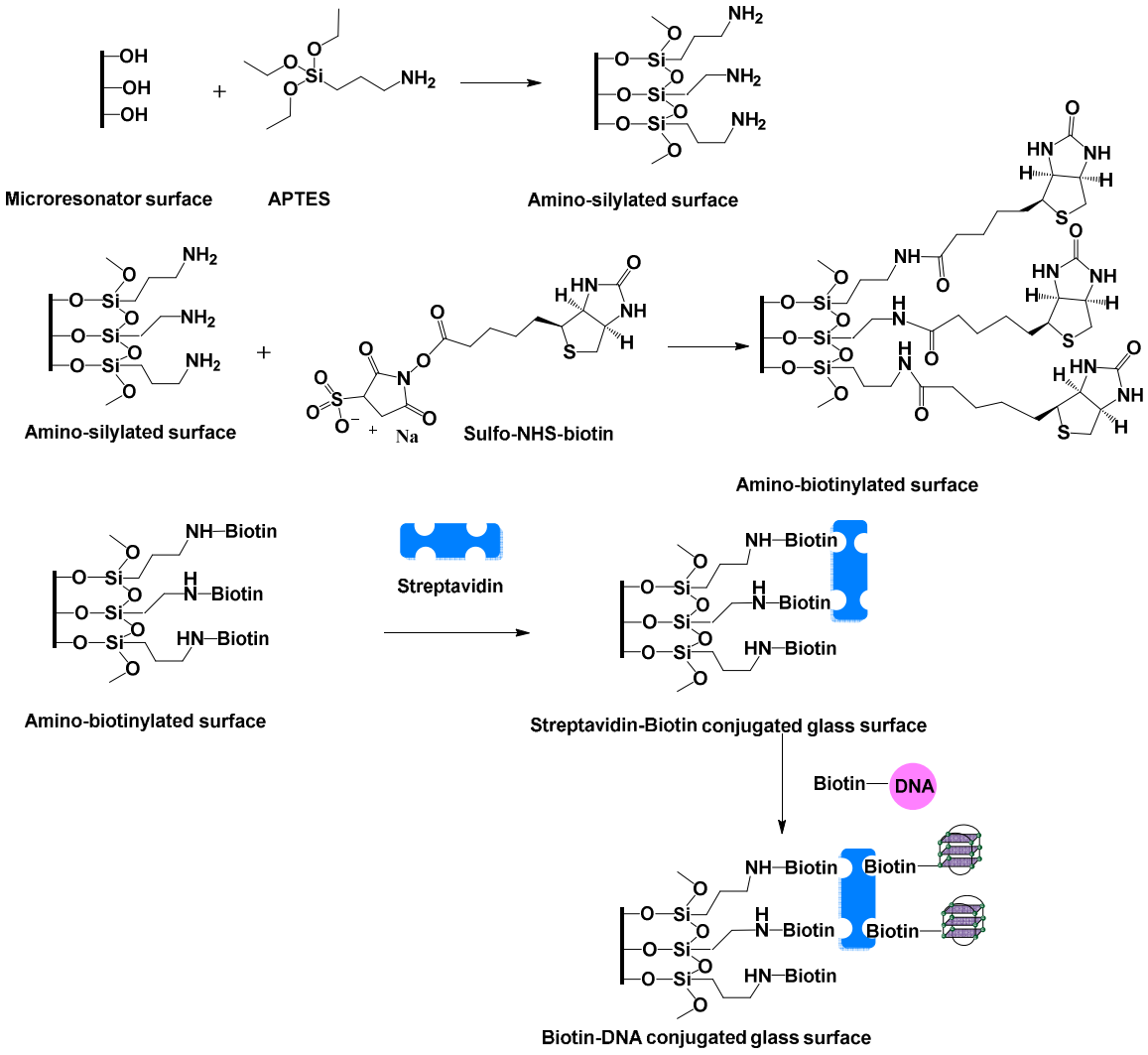

Figure S1. General synthetic strategy for microresonator surface modification.

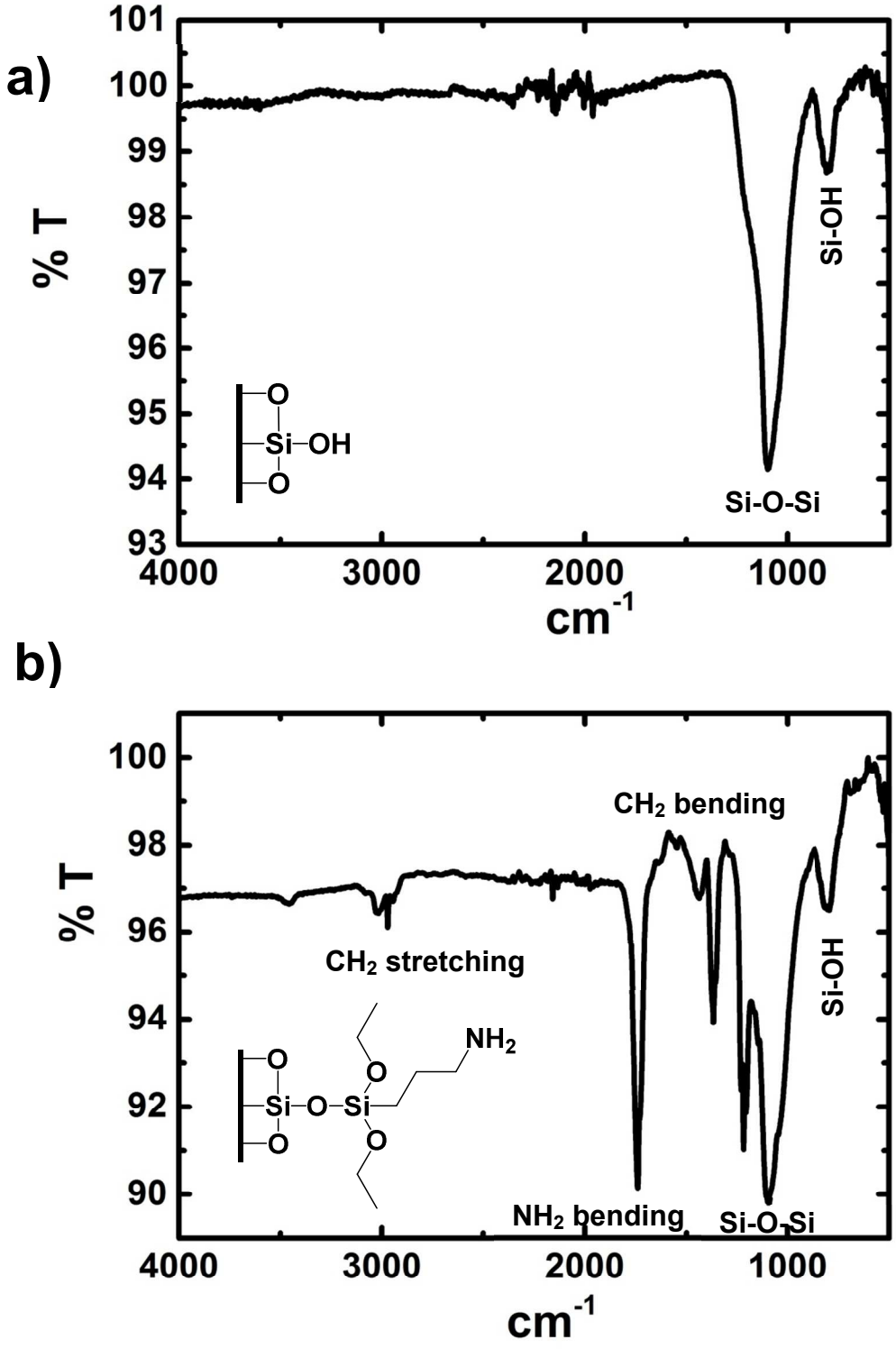

Figure S2. AT-IR characterization of microresonators before (a) and after (b) APTES functionalization

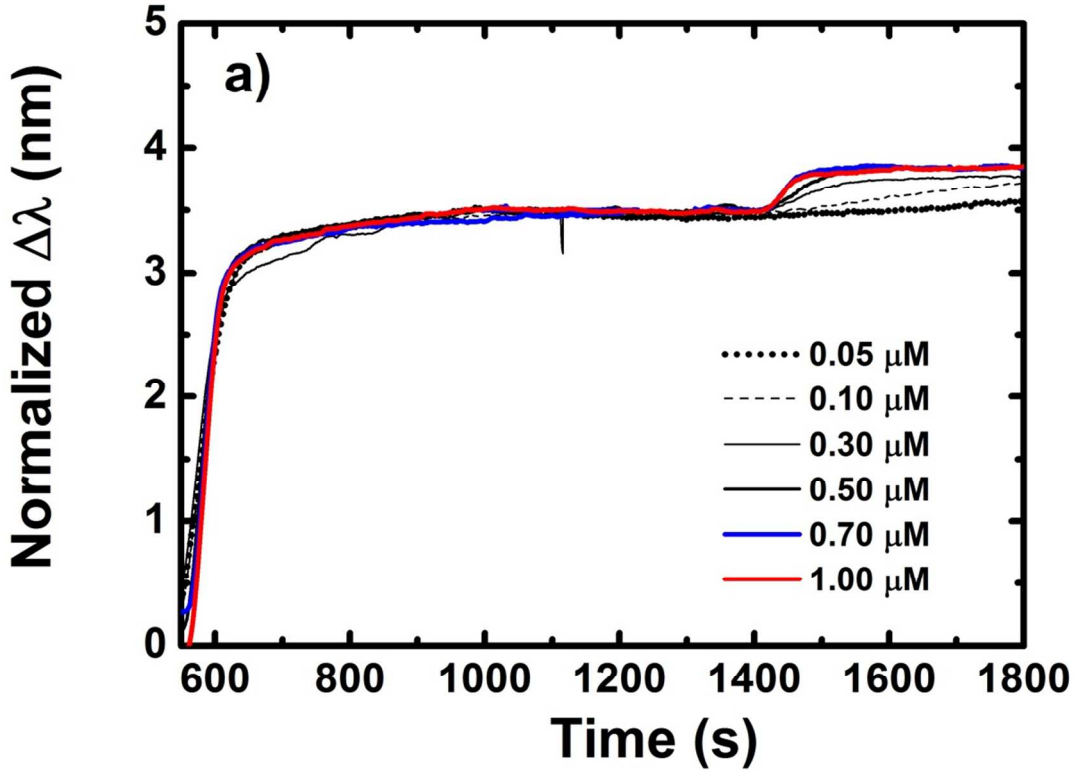

Figure S3. WGM real time monitoring of the immobilization of prefolded c-myc G4 DNA onto a resonator using increasing DNA concentrations (0.05-1.00 μM).

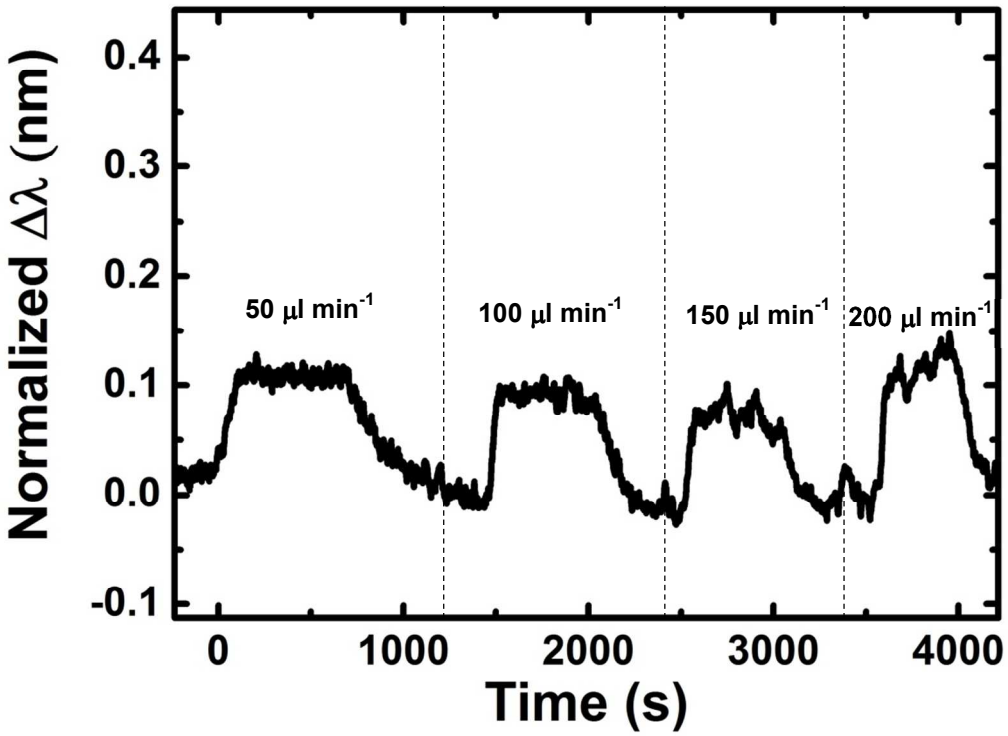

Figure S4. Kinetic analysis of the interaction between CV and c-myc G4 DNA immobilized on a WGM resonator at different flow rates. CV concentration was 1.5 μM and flow rate varied between 50-200 $\mu L.min^{-1}$. The normalized $\Delta\lambda$ was found to be independent from the flow rate indicating that binding is not limited by mass transport.

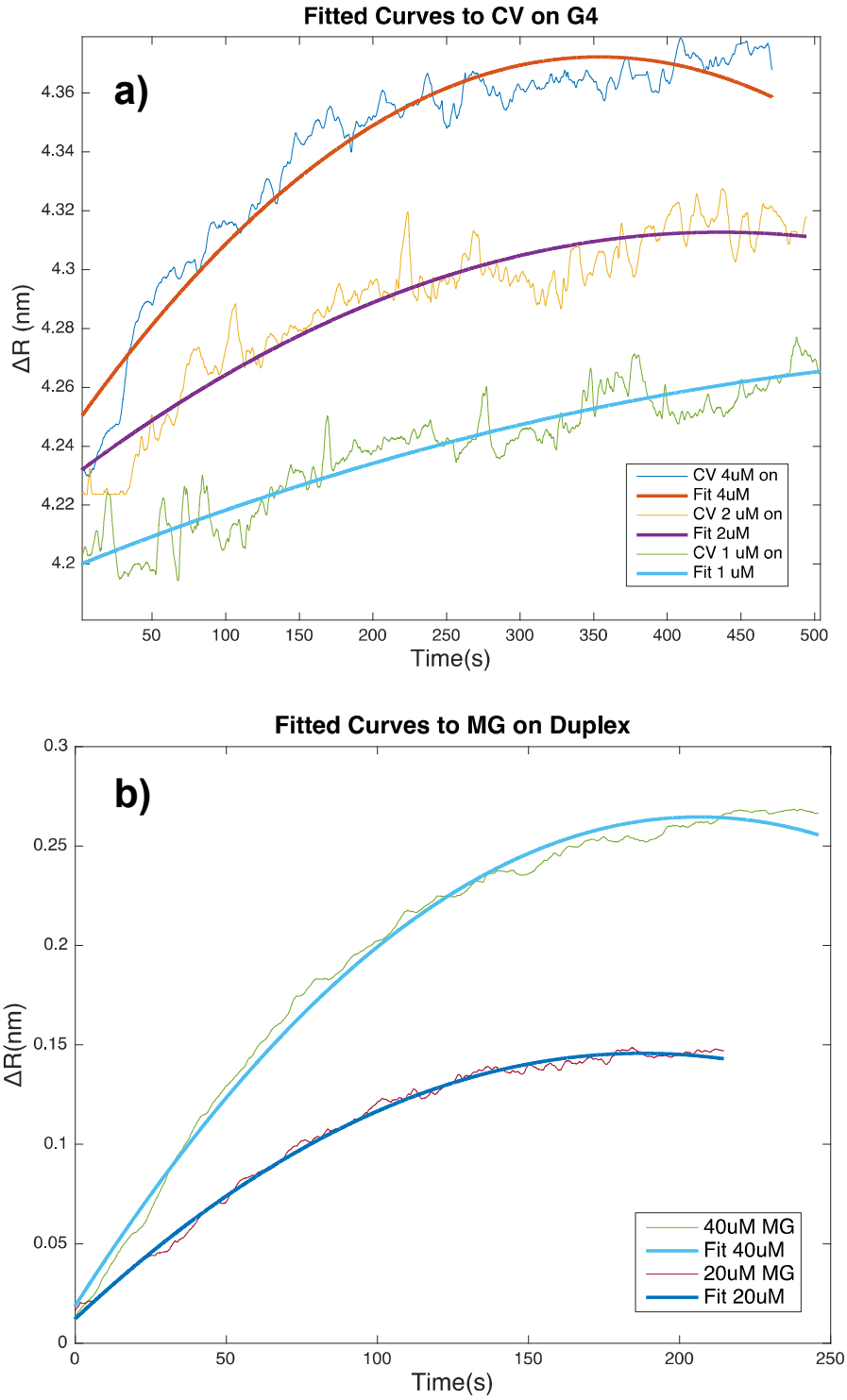

Figure S5. Illustration of two-term polynomial fit curves onto a) CV on G4 and b) MG on Duplex. Polynomial equation is f(x) = p1*x^2 + p2*x + p3. P1= K_{obs}.

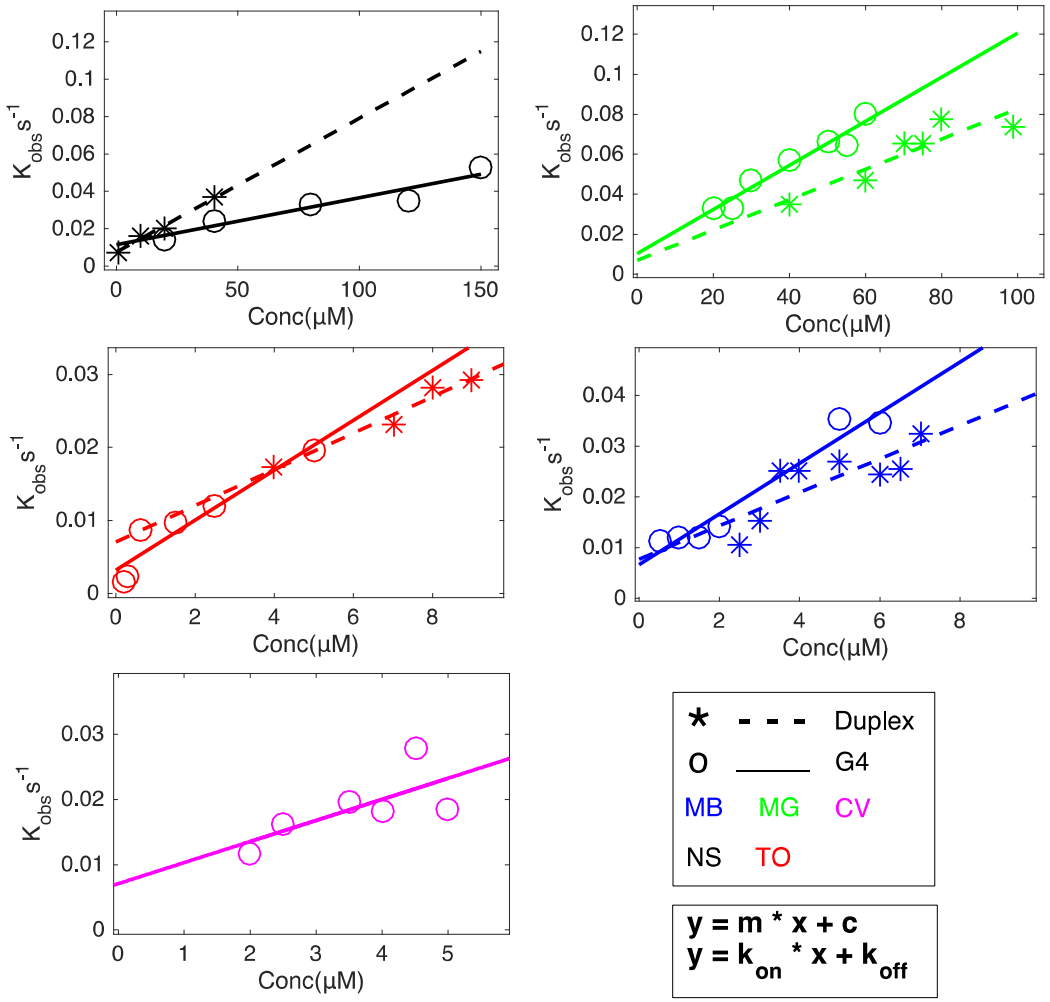

Figure S6. Plot of WGM k_{obs} as a function of ligand concentration. Illustrates K_{on} (gradient) and k_{off} (intercept) – values listed in Table 1.

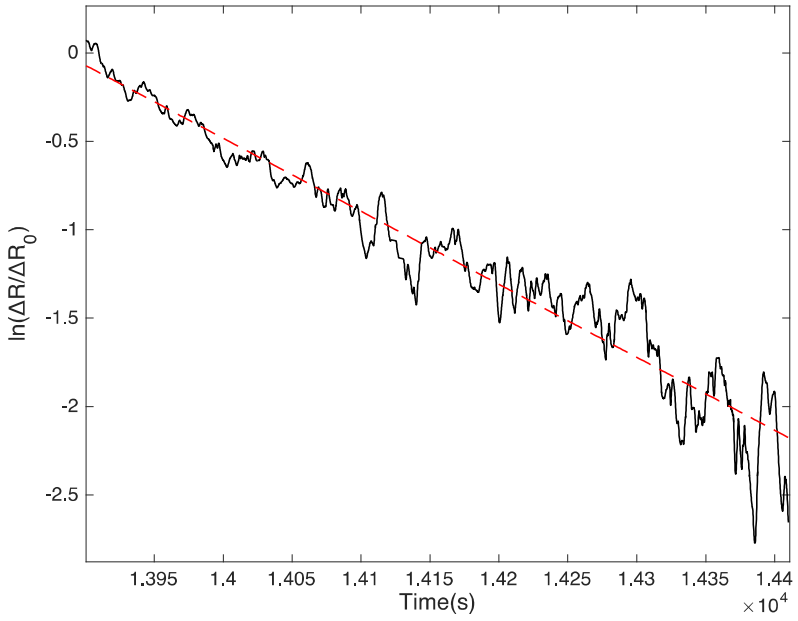

Figure S7. Linear fit of $\ln(\Delta R/\Delta R_0)$ during the dissociation phase of the curve. 4µM CV dissociates from a G quadruplex-coated resonator after injection of buffer at a flow rate of 100µl/min.

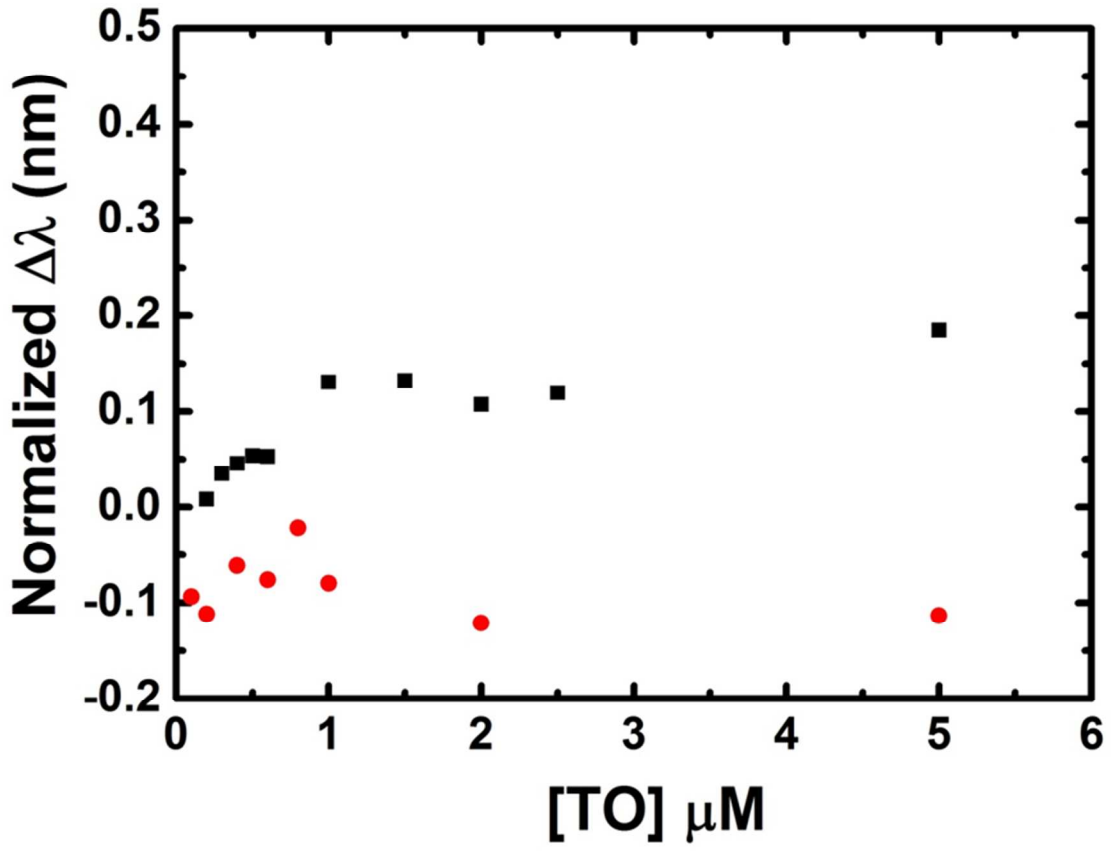

Figure S8. Normalized wavelength shifts for binding of TO to either a bare WGM resonator (red circles) or to a WGM resonator functionalized with the c-myc G4 DNA (black squares).

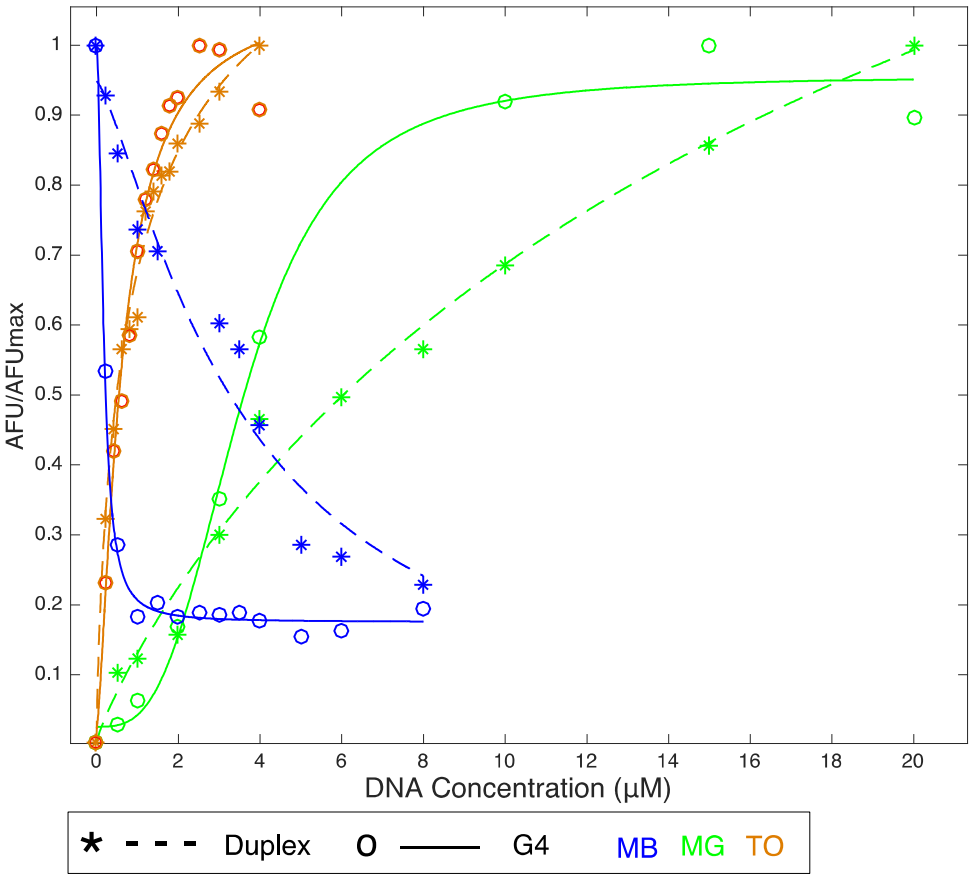

Figure S9. Fluorescent titration control experiments. Fraction bound of different ligands in AFU with G4 and duplex DNA, in order to estimate K_D at EC50. NB: MB fluorescence decreases with DNA addition.

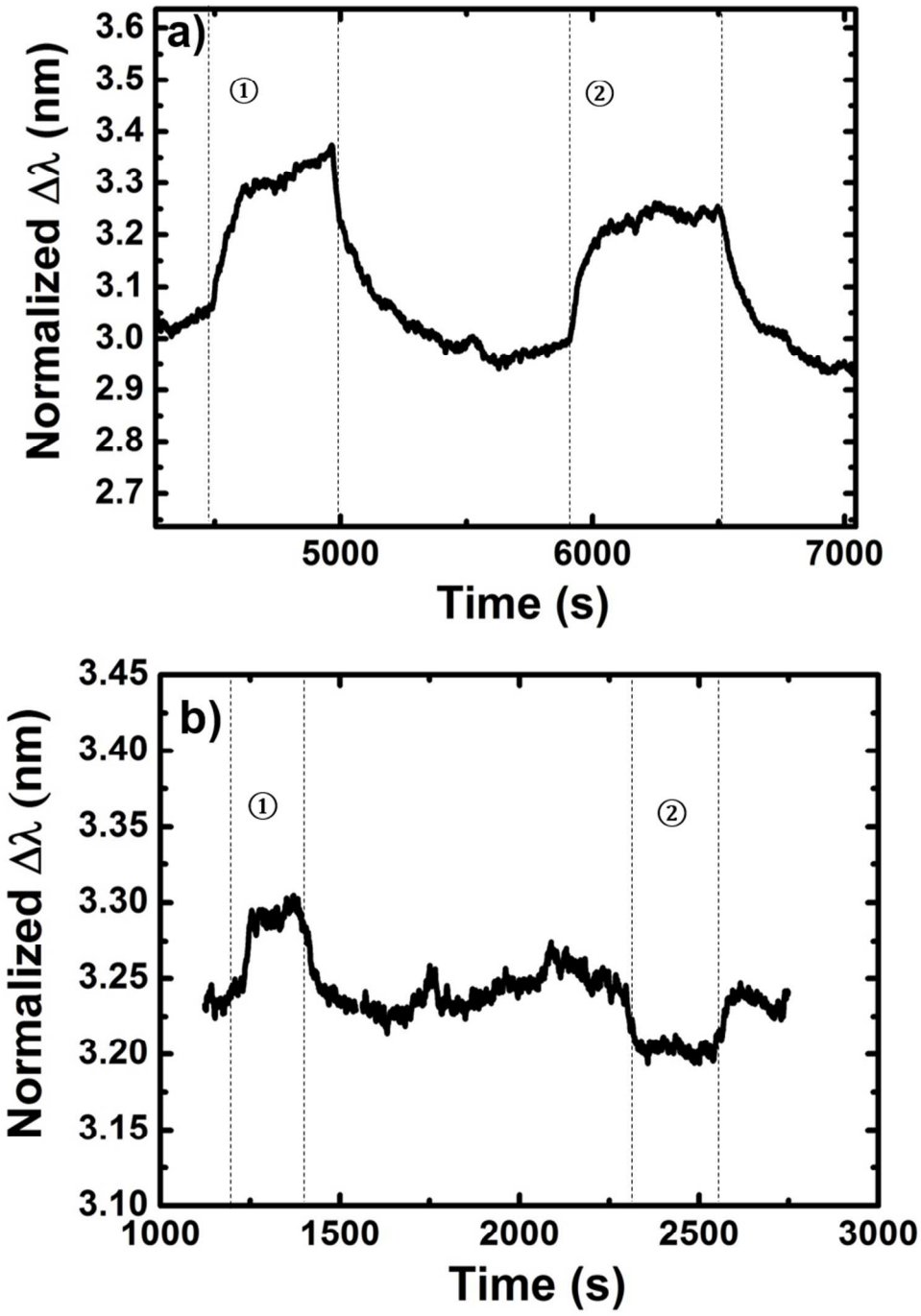

Figure S10. Quadruplex/duplex DNA competition experiments. WGM resonators were functionalized with prefolded cmyc G4 DNA. Binding of CV (a) and MB (b) to the G4 DNA was then monitored in real time in the absence (①) and in the presence (②) of competitor double-stranded CT DNA.

DNA	G quadruplex		Duplex	
	K_{off} (s^{-1})	K_{off} (s^{-1})	K_{off} (s^{-1})	K_{off} (s^{-1})
Ligand	Intercept	Log dissoc.	Intercept	Log dissoc.
CV	0.00710	0.00597	*	*
MB	0.00980	0.01315	0.00897	0.00710
TO	0.00149	0.00139	0.00705	0.00528
MG	0.01031	0.0173	0.01865	0.00866
NS	0.01140	0.0134	0.00754	****

Table S1. Two sets of independently calculated k_{off} values. One set is deduced from the log-transformed dissociation slopes, according to the protocols of Soteropulos et al (2011). These are presented alongside the k_{off} values obtained from the intercept of the observed association constants k_{obs}.

Values could not be estimated because (*) the transmission spectrum was perturbed by high polarizability; (***) ≤3 dissociation slopes available for analysis.

DNA Ligand	G quadruplex Fluorescent K_D (μM)	Duplex Fluorescent K_D (μM)
CV	**	**
MB	0.19	3.09
TO	0.63	1.03
MG	3.56	>20
NS	***	***

Table S2. Dissociation constant K_D values calculated by fluorescence titration experiments. Values could not be estimated because (**) data range did not fit a dose response curve; (***) molecule was not fluorescent.